

PAPER

Twist effects in quantum vortices and phase defects

To cite this article: Simone Zuccher and Renzo L Ricca 2018 *Fluid Dyn. Res.* **50** 011414

View the [article online](#) for updates and enhancements.

Related content

- [A vortex filament tracking method for the Gross–Pitaevskii model of a superfluid](#)
Alberto Villois, Giorgio Krstulovic, Davide Proment et al.
- [Scaling properties towards vortex reconnection under Biot–Savart evolution](#)
Y Kimura and H K Moffatt
- [Helicity and topology of a small region of quantum vorticity](#)
M Mesgarnzhad, R G Cooper, A W Baggaley et al.

Twist effects in quantum vortices and phase defects

Simone Zuccher^{1,4}  and Renzo L Ricca^{2,3} 

¹ Department of Computer Science, U. Verona, Ca' Vignal 2, Strada Le Grazie 15, I-37134, Verona, Italy

² Department of Mathematics and Applications, U. Milano-Bicocca, Via Cozzi 55, I-20125, Milano, Italy

³ BDIC, Beijing U. Technology, 100 Pingleyuan, Beijing 100124, People's Republic of China

E-mail: simone.zuccher@univr.it and renzo.ricca@unimib.it

Received 28 December 2016, revised 18 July 2017

Accepted for publication 21 July 2017

Published 3 January 2018



CrossMark

Communicated by Professor Yasuhide Fukumoto

Abstract

In this paper we show that twist, defined in terms of rotation of the phase associated with quantum vortices and other physical defects effectively deprived of internal structure, is a property that has observable effects in terms of induced axial flow. For this we consider quantum vortices governed by the Gross–Pitaevskii equation (GPE) and perform a number of test cases to investigate and compare the effects of twist in two different contexts: (i) when this is artificially superimposed on an initially untwisted vortex ring; (ii) when it is naturally produced on the ring by the simultaneous presence of a central straight vortex. In the first case large amplitude perturbations quickly develop, generated by the unnatural setting of the initial condition that is not an analytical solution of the GPE. In the second case much milder perturbations emerge, signature of a genuine physical process. This scenario is confirmed by other test cases performed at higher twist values. Since the second setting corresponds to essential linking, these results provide new evidence of the influence of topology on physics.

Keywords: twist, vortex rings, quantum vortices, phase defects, helicity

(Some figures may appear in colour only in the online journal)

⁴ Author to whom any correspondence should be addressed.

1. Introduction

Quantum vortices are physical realizations of phase singularities that emerge in a disparate variety of physical systems, including superfluid Helium, Type-II superconductors, photon fields (optical vortices) and atomic gases such as Bose–Einstein condensates (Nelson 2002). In this paper we investigate twist effects by focusing on quantum vortices that evolve under the 3D Gross–Pitaevskii equation (GPE) (Pitaevskii 1961, Gross 1963)

$$\frac{\partial \psi}{\partial t} = \frac{i}{2} \nabla^2 \psi + \frac{i}{2} (1 - |\psi|^2) \psi, \quad (1)$$

for the complex wave function ψ with background unit density ($|\psi|^2 \rightarrow 1$ as $|\mathbf{x}| \rightarrow \infty$). It is well-known that these defects are actually one-dimensional phase singularities in the order parameter of the ambient space, carrying angular momentum. They can be thought of as infinitesimally thin, empty tubes centered on a space curve (the tube centerline). These tubes are regions effectively deprived of internal structure, having zero density and vorticity given by a delta-function on the axis. Hence, a mathematical definition of twist seems lacking of physical interpretation. However, our recent work on helicity change due to interaction and reconnection of quantum vortex loops (Zuccher and Ricca 2015, 2017) has shown that twist, appropriately defined, has physically observable effects. Scope of the present paper is to clarify and investigate further the origin of twist and its physical manifestation in the context of GPE quantum vortex interactions and to extend these new findings to other physical phase defects.

Twist is a fundamental ingredient in the kinetic helicity of classical vortex filaments. Helicity \mathcal{H} is a conserved quantity of ideal fluid mechanics (Moreau 1961) given by the volume integral of the scalar product of velocity \mathbf{u} and vorticity $\boldsymbol{\omega} = \nabla \times \mathbf{u}$. When vorticity is confined to n vortex tubes of equal circulation Γ (as in the case of quantum vortices) \mathcal{H} can be simplified and reduced to a sum of linking numbers (Moffatt 1969, Moffatt and Ricca 1992, Ricca and Moffatt 1992). By taking $\overline{\mathcal{H}} = \mathcal{H}/\Gamma^2$, we have

$$\overline{\mathcal{H}} = \sum_{i \neq j}^n Lk_{ij} + \sum_i^n SL_i, \quad (2)$$

where Lk_{ij} denotes the Gauss linking number between vortices i and j , and SL_i denotes the Călugăreanu–White self-linking number of the single i -vortex. For closed filaments Lk and SL are both topological invariants given by pure integers; moreover, SL can be written as sum of writhe Wr and twist Tw , two global geometric quantities given by real numbers (see section 2.1 for definitions). Detailed study of these geometric and topological quantities provides insight into the dynamics and energetics of complex systems and are therefore useful to understand and interpret physical aspects as well (Ricca and Berger 1996, Moffatt 2014).

As we shall see, writhe is a geometric property of the vortex axis, so it is well-defined as long as one can identify the geometry of the tube centerline. Twist, however, is not a geometric property of a single space curve, but rather of a ribbon defined by a pair of neighboring curves winding one around the other. In the case of a classical vortex one can think of twist as the result of the winding of any pair of vortex lines in a coherent bundle of vorticity. Not so for quantum vortices, where there are no field lines to refer to. On the basis of the mathematical definitions given below (section 2.1) we propose to define twist in terms of the winding of the phase of the wave function around the defect line and explore the physical implications that this twist has in the dynamics of the system. This investigation is carried out by a series of numerical simulations based on different initial conditions

(section 3) and analysis of the corresponding evolution. The results are presented in section 4 and concluding remarks are drawn in section 5.

2. Governing equations, basic definitions and twist interpretation

The GPE (1) is commonly employed to model and study quantum vortex reconnection (Koplik and Levine 1993, Zuccher *et al* 2012, Allen *et al* 2014) under conservation of the Hamiltonian $E = K + I$, given by the sum of kinetic energy $K = \frac{1}{2} \int \nabla \psi \cdot \nabla \psi^* d^3\mathbf{x}$ and interaction energy $I = \frac{1}{4} \int (1 - |\psi|^2)^2 d^3\mathbf{x}$ (where ψ^* denotes the ψ complex conjugate). By using the Madelung transformation $\psi = \sqrt{\rho} \exp(i\theta)$, where θ is the phase of the wavefunction, equation (1) admits fluid mechanical interpretation in terms of the standard continuity equation and momentum equation. By taking real and imaginary parts we have

$$\frac{\partial \rho}{\partial t} + \frac{\partial(\rho u_k)}{\partial x_k} = 0, \quad (3)$$

$$\rho \left(\frac{\partial u_k}{\partial t} + u_l \frac{\partial u_k}{\partial x_l} \right) = - \frac{\partial p}{\partial x_k} + \frac{\partial \tau_{kl}}{\partial x_l}, \quad (4)$$

where $\rho = |\psi|^2$ is fluid density, $\mathbf{u} = \nabla \theta$ velocity, $p = \rho^2/4$ pressure and $\tau_{kl} = \frac{1}{4} \rho \frac{\partial^2 \ln \rho}{\partial x_k \partial x_l}$ ($k, l = 1, 2, 3$) the so-called quantum stress. This latter term is negligible with respect to the quantum pressure term at length scales much larger than the healing length ξ , that is of the order of the vortex core radius (Zuccher *et al* 2012). According to the normalization used in equations (3) and (4) we take $\xi = 1$ and quantum of circulation $\Gamma = 2\pi$.

2.1. Standard definitions of geometric and topological properties

As physical singularities of vorticity, quantum vortices can be regarded as zero density lines where phase is ill-defined. We identify the phase singularity with the vortex centerline C . Let's briefly recall the standard definition of the topological and geometric quantities present in equation (2). The linking number between vortex i and j is given by the double integral over the centerlines C_i and C_j , given by

$$Lk_{ij} = \frac{1}{4\pi} \int_{C_i} \int_{C_j} \frac{\mathbf{X}_i - \mathbf{X}_j}{\|\mathbf{X}_i - \mathbf{X}_j\|^3} \cdot (d\mathbf{X}_i \times d\mathbf{X}_j), \quad (5)$$

where \mathbf{X}_i and \mathbf{X}_j denote the position vectors of two points, respectively on C_i and C_j ($i \neq j$). Lk_{ij} is a topological invariant of the link. It takes only integer values and provides a measure of the degree of linking of two (or more) components, contributing to the 'external' helicity of a link of two or more vortices.

The writhing number Wr_i contributes to the 'internal' helicity through the self-linking number $SL_i = Wr_i + Tw_i$ of each individual vortex. The writhe is defined by

$$Wr_i = \frac{1}{4\pi} \int_{C_i} \int_{C_i} \frac{\mathbf{X}_i - \mathbf{Y}_i}{\|\mathbf{X}_i - \mathbf{Y}_i\|^3} \cdot (d\mathbf{X}_i \times d\mathbf{Y}_i), \quad (6)$$

where \mathbf{X}_i and \mathbf{Y}_i denote two distinct points on the same curve C_i . Wr_i is a global geometric property of C_i , taking real values. A plane curve has writhe always zero, but sometimes even fully twisted space curves may have writhe equal to zero, when positive and negative writhe contributions compensate. Since writhe takes into account distortion, in general it is a good indicator of three-dimensional folding.

Total twist T_{w_i} is the other global geometric ingredient of SL_i . Its definition is based on the concept of ribbon. A mathematical ribbon $R = R(C, C^*)$ of width ϵ is defined by prescribing a baseline curve C (one edge of the ribbon) of vector equation $\mathbf{X}(s)$ and a second curve C^* (the other edge of R) of vector equation $\mathbf{X}^*(s)$ given by $\mathbf{X}^*(s) = \mathbf{X}(s) + \epsilon \hat{\mathbf{U}}(s)$, where s is arc-length and $\hat{\mathbf{U}}$ denotes a normal unit vector to \mathbf{X} . Hence, for the i vortex of centerline C_i and ribbon R_i , the total twist number is defined by the rate of rotation of $\hat{\mathbf{U}}$ around the base curve C_i , i.e.

$$T_{w_i} = \frac{1}{2\pi} \int_{C_i} \left(\hat{\mathbf{U}} \times \frac{d\hat{\mathbf{U}}}{ds} \right) \cdot d\mathbf{X}_i. \quad (7)$$

Total twist can be further decomposed $T_{w_i} = T_i + N_i$ in terms of normalized total torsion T_i and intrinsic twist N_i (Moffatt and Ricca 1992, Ricca and Moffatt 1992), given respectively by

$$T_i = \frac{1}{2\pi} \int_{C_i} \tau(s) ds \quad (8)$$

and

$$N_i = \frac{1}{2\pi} \int_{C_i} \frac{d\Theta(s)}{ds} ds = \frac{[\Theta]_{C_i}}{2\pi}, \quad (9)$$

where $\tau = \tau(s)$ is torsion of C_i , and $\Theta = \Theta(s)$ the angle between $\hat{\mathbf{U}}$ and the principal unit normal $\hat{\mathbf{N}}$ to C_i . T_i takes real values and is evidently zero for straight lines and planar curves; N_i is an integer (if C_i is a closed curve) measuring the total number of full turns of $\hat{\mathbf{U}}$ all along C_i relative to the Frenet triad on C_i ; it can be visualized by a twisted straight ribbon whose axis has zero torsion.

Since GPE vortices (and other physical phase defects) have no internal structure and are fibered by smooth iso-phase surfaces (Seifert surfaces), we can unambiguously evaluate twist by using directly equation (7) (rather than (8) and (9)). This is done by identifying the rotation of $\hat{\mathbf{U}}$ with the rotation of one of these iso-phase surfaces around the defect line. By introducing the concept of ribbon we implement a technique introduced in earlier work (Zuccher and Ricca 2015) and applied again recently (Zuccher and Ricca 2017). A reference ribbon R_i is defined by taking the vortex axis C_i as the baseline curve of R_i and a second curve C_i^* on the given iso-phase surface $\theta = \bar{\theta}$ of our choice. The ribbon is then identified by the points of constant phase that lie on the ϵ -portion of this iso-phase surface $\theta = \bar{\theta}$ bounded by C_i and C_i^* . Twist is then measured by the full rotation of this ribbon around C_i , that by construction amounts to the full rotation of $\hat{\mathbf{U}}$ around the defect line. A phase contour associated with a planar vortex ring with $Wr = 0$ and $T = N = Tw = 0$ is visualized in the (y, z) -plane at $x = 0$ in figure 1. The phase discontinuity between $\theta = -\pi$ and $\theta = \pi$, where the value jumps (from blue to red, online) due to the multiple-connectivity of the ambient space, is visible in the region exterior to the ring. Any choice of framing, provided for example by $\hat{\mathbf{U}}$ in the $\theta = \bar{\theta} = 0$ direction is independent of both the geometry of the curve and the intrinsic Frenet triad on C_i . The use of these iso-phase Seifert surfaces allows computation of helicity via direct computation of its geometric and topological ingredients and provides an alternative route to the computation of helicity based on regularization techniques and high-order derivatives (Clark di Leoni *et al* 2016).

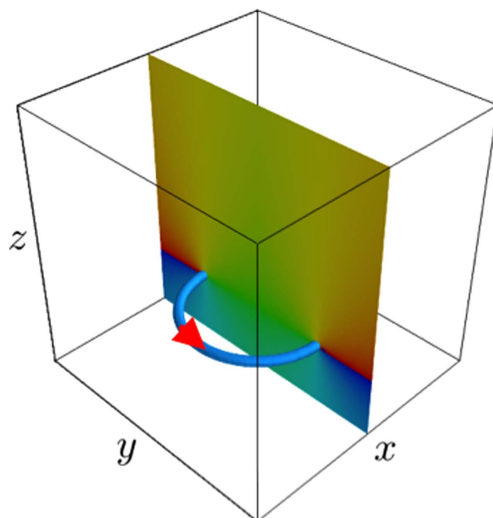


Figure 1. Planar vortex ring with $Wr = 0$, $T = N = 0$ (hence $Tw = 0$) and phase contour in the (y, z) -plane at $x = 0$. The arrow indicates the vorticity direction. Values of phase change according to color, with an evident phase discontinuity from $\theta = -\pi$ to $\theta = \pi$ (from blue to red, online). In the interior region the vortex is spanned by the iso-phase surface $\theta = 0$ (not visualized), that is a Seifert surface given by the circular disk D bounded by the ring axis $C = \partial D$. Any given iso-phase surface provides a well-defined framing on C .

2.2. Physical interpretation of twist

Since defects have topological charge (circulation) quantized, phase can only take discrete, integer values, so that twist, defined in terms of phase rotation through θ , can only take integer values as well. This is a first, fundamental difference between classical and quantum systems. Moreover when N quantum vortices are simultaneously present, they would normally have unit circulation (normalized in terms of Planck constant and particle mass), a necessary condition for stability. This poses an additional, global constraint on the whole system. Hence, phase values are not only individually locked to discrete values, but these values cannot vary arbitrarily, and this is a second fundamental difference between classical and quantum systems.

Twist has physical implications through its phase definition and the relation of phase with velocity $\mathbf{u} = \nabla\theta$. First, note that any choice of $\theta = \bar{\theta}$ is uninfluential in twist computation, since only gradients of phase matter. The effect of twist is made clear if we interpret it in terms of the corresponding velocity decomposed locally in cylindrical polar coordinates (r, ϕ, z) centered on a straight vortex axis C . If the iso-phase surface $\theta = \bar{\theta}$ is not twisted, it simply coincides with the coordinate plane $\phi = \bar{\theta}$. The gradient, normal to this surface, gives rise to the velocity $\mathbf{u} = (0, u_\phi, 0)$ with $u_\phi = \Gamma/2\pi r$ (r distance from the tube axis), in analogy with the classical rectilinear vortex filament solution. In the stationary case the family of iso-phase surfaces fiber the ambient space by a fan of straight planes hinged on C , with streamlines given by concentric plane circles. Hence, by construction local twist is non-zero only when the gradient of the phase has a component directed along C , and since $\mathbf{u} = \nabla\theta$ twist is directly related to the axial component of the velocity along C . This makes twist effects observable and measurable. Physical effects associated with phase are therefore all

important and cannot be neglected by simply reducing the evolution of a quantum vortex, or indeed of any phase defect, to the motion of a line singularity. Particularly so, for instance, in relation to helicity computation. Moreover, as in the classical case, the simultaneous presence of a number of vortices determine a superimposition of the induced effects that in the quantum case is evidenced by phase rotations. This has been investigated by considering the simultaneous presence of two linked, planar vortex rings (constituting a Hopf link) that determine a mutually induced phase twist on each individual vortex as signature of the complex topology of the system (Zuccher and Ricca 2017).

3. Numerical method

GPE (1) is integrated numerically by employing the well-known second-order Strang splitting Fourier spectral method (Koplik and Levine 1993), that has been consistently used for numerical simulations of vortex reconnection (Zuccher *et al* 2012, Allen *et al* 2014, Zuccher and Ricca 2015, Caliarì and Zuccher 2017). Its main advantages are that mass conservation is enforced *exactly* and efficiency is guaranteed by fast Fourier transform algorithms. Exact mass conservation will be particularly important in the diagnostics and interpretation of the results presented below. The main drawback is that non-periodic initial conditions must be made triply periodic by doubling the computational domain in each direction by introducing mirror vortices, a technique that has been extensively employed in literature (Koplik and Levine 1993).

3.1. Initial conditions

We want to study the effect of twist under different initial conditions in the simplest possible scenario in order to understand and explore the dynamical response of the system to natural or artificial settings. For this purpose a planar vortex ring of radius $R = 8$, circulation $\Gamma = 2\pi$ and zero twist is placed parallel to the (x, y) -plane. As was done in Zuccher and Ricca (2017), the density distribution in the plane orthogonal to the vortex central axis is prescribed by the high-order Padé approximation $\rho_0(r) = \frac{a_1 r^2 + a_2 r^4 + a_3 r^6 + a_4 r^8}{1 + b_1 r^2 + b_2 r^4 + b_3 r^6 + a_4 r^8}$ (see Caliarì and Zuccher 2016 for details), and the initial phase is eventually let to change by 2π in that plane (see figure 1). At $t = 0$ the resulting wave function is thus given by $\psi_0 = \sqrt{\rho_0} \exp(i\theta_0)$. Since the ring travels in the positive z -direction (upward), the ring is initially placed below the plane $z = 0$.

The computational domain is given by $[-15; 15] \times [-15; 15] \times [-15; 15]$ and it is chosen to optimize the observed vortex evolution. The spatial discretization is the same in each direction (as in former simulations by Zuccher and Ricca 2015, 2017), with resolution $\Delta x = \Delta y = \Delta z = \xi/3$, 90^3 grid points in the physical domain (before mirroring) and time step $\Delta t = 1/80 = 0.0125$.

To superimpose twist on the ring of figure 1, we *make* rotate uniformly the phase through θ by 2π along C . The result is shown in figure 2(a), where the jump in phase between $-\pi$ and π rotates uniformly around C , all along C . This twist prescription, however, results rather unphysical, because it is inconsistent with the uniform, initial density distribution, left unchanged. Careful data analysis and close inspection of the phase relaxation show that the constraints imposed by $\rho = |\psi|^2 = 1$ and the exact mass conservation enforced by the numerical code determine a forced adaptation of the background density with subsequent generation of a secondary, central phase defect and an induced change of θ by 2π along the z -axis. This is accompanied by the production of spurious waves that propagate away from the vortex towards the boundaries, bouncing back to the numerical domain.

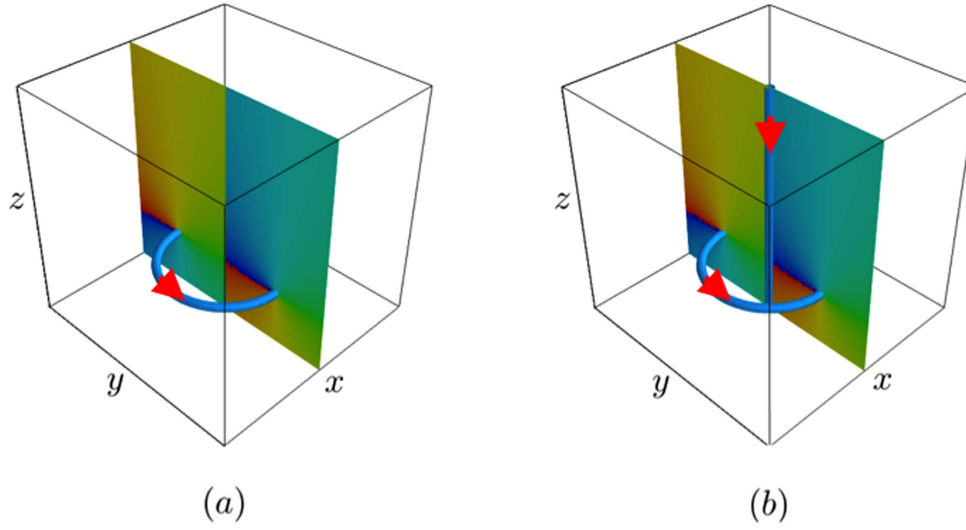


Figure 2. Phase contours in the (y, z) -plane for a planar ($T=0$) vortex ring with $T_w (=N) = 1$. (a) Twist is artificially superimposed by rotating the phase by 2π uniformly all along the vortex centerline. (b) The same twist $T_w = 1$ is naturally induced by the presence of a rectilinear vortex with vorticity along the negative z -direction (downwards). The vortex tubes of core radius a are visualized by iso-density surfaces, with $\rho = 0.1$ and $a \approx \xi/2$.

All this suggests to test a different initial condition given by a vortex ring with $T_w = 0$ (as in figure 1) and a rectilinear vortex placed along the central axis of the ring with vorticity pointing in the negative direction of the z -axis (downwards). The phase contour is shown in figure 2(b) together with the vortex tubes. In this case we have $\psi_0 = \sqrt{\rho_{01}\rho_{02}} \exp[i(\theta_{01} + \theta_{02})]$ (subscripts refer to the vortex ring and the straight vortex, respectively). The density distribution of the straight vortex is calculated by using the high-order Padé approximation mentioned above, with the phase change obtained by rotating θ_2 around the z -axis. This rotation is measured by the winding number w , so that $\psi_0 = \sqrt{\rho_0} \exp(iw\theta_0)$. The density distribution of a straight vortex with $w > 1$ must be computed numerically by solving the nonlinear boundary value problem

$$f''(r) + \frac{1}{r}f'(r) + \left[1 - f^2(r) - \frac{w^2}{r^2}\right]f(r) = 0, \quad (10)$$

with boundary conditions $f(0) = 0$, $f(\infty) = 1$ and $f(r) = \sqrt{\rho(\sqrt{x^2 + y^2})}$. An efficient method for solving (10) is described in Caliari and Zuccher (2016). Note that the iso-density surface of the core radius of the straight vortex increases with the winding number w .

4. Results

Figure 3 shows initial condition and solution at $t = 20$ for the case of a twisted vortex ring obtained by superimposing a full turn of the phase ($T_w = N = 1$) on the initial ring. A straight, central vortex is immediately produced from the first time step, as a result of a competition between barotropic and quantum pressure (see equation (4)). At the beginning the diameter of this vortex (in terms of density distribution) is quite small, but then it adjusts

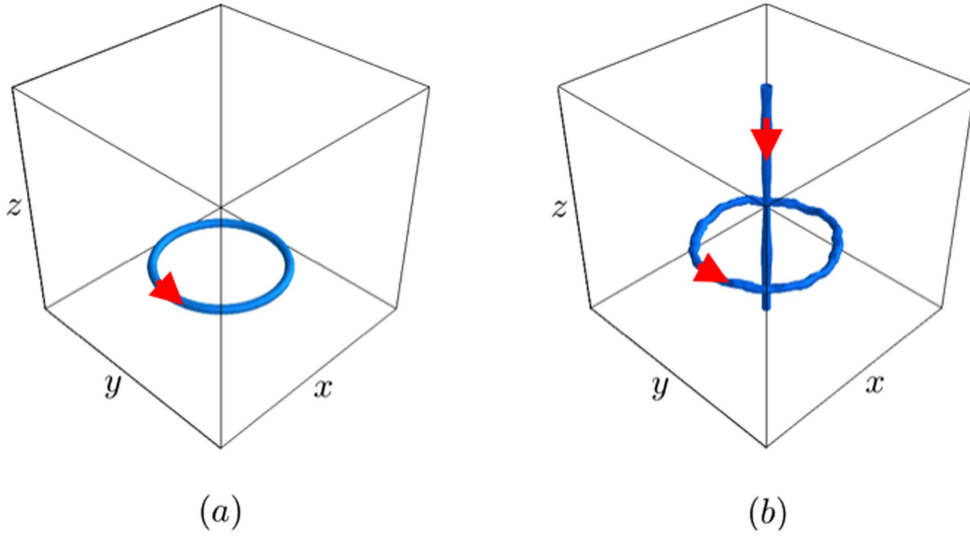


Figure 3. (a) Initial condition $t = 0$: twist $T_w = 1$ is superimposed on the vortex ring by artificially rotating around the vortex axis the iso-phase surface $\theta = \bar{\theta}$ by 2π . (b) $t = 20$: a central, straight vortex is instantly produced from the very first time-step. The iso-density surfaces ($\rho = 0.1$ and $a \approx \xi/2$) appear highly corrugated.

to the value given by the Padé approximation. Perturbations develop quickly by corrugating the iso-density surfaces of the ring and the central vortex with growing amplitude (see figure 3(b)). Further tests confirm that the observed irregularities are due to artificial conditions and the perturbations persist till a complete, progressive relaxation of any density inhomogeneity. Test cases (not shown here) have been run by placing an initially straight phase defect in a uniform background density $\rho = 1$, so as to reproduce the same phase distribution given by a straight vortex. As discussed earlier, a real vortex emerges showing an irregular iso-density surface from the very first time step. We believe that this irregularity is due to the artificial forcing of the numerical solution to the GPE equation. Evidently this forcing generate perturbations that, similarly to sound emission, propagate away from the phase singularity and by nonlinear interaction with other perturbations produce widespread density fluctuations.

Figure 4 shows initial condition and solution at $t = 20$, when a vortex ring and a straight, central vortex are prescribed as initial conditions. In this case we observe much milder and regular perturbations that most likely are ascribed to real physical effects due to the presence of axial flow. The induced perturbations due to the action of an axial flow is a well-known mechanism that has been subject of intense study in the context of classical vortex filament dynamics (Widnall and Bliss 1971, Moore and Saffman 1972, Fukumoto and Miyazaki 1991). We believe that the oscillations of figure 4(b) are indeed due to the action of axial flows.

It is interesting to compare the intensity of the induced axial velocity u_a evaluated at points on the vortex ring core with the propagation speed U of the vortex ring, and provide a crude estimate on possible instabilities based on direct inspection of figure 4(b). In our case we have $\Gamma = 2\pi$, vortex ring radius $R = 8$ and core radius $a \approx \xi/2 = 1/2$. The axial velocity u_a is that due to the straight central vortex at points on the vortex ring core placed at distance $r = R - a$ from the z -axis; thus

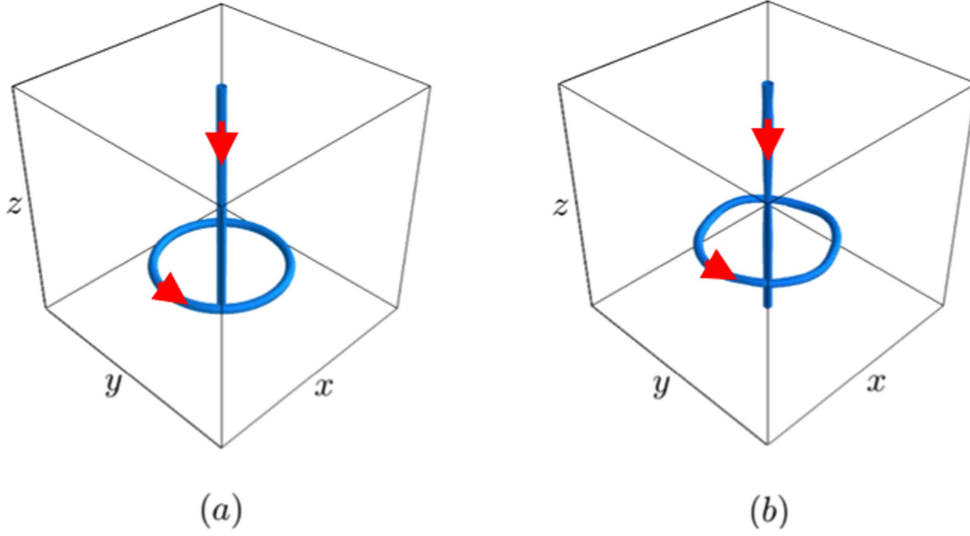


Figure 4. (a) Initial condition $t = 0$: a vortex ring and a straight central vortex are initially present; both vortices have zero initial twist. The central vortex induces a unit twist on the ring (see the contour plot of figure 2(b)). (b) $t = 20$: in this case the isodensity surfaces ($\rho = 0.1$ and $a \approx \xi/2$) are rather regular.

$$u_a \equiv u_\phi = \frac{\Gamma}{2\pi(R - a)}. \quad (11)$$

The speed U is given by Sullivan *et al* (2008)

$$U = \frac{\Gamma}{4\pi R} \left(\ln \frac{8R}{a} - \frac{1}{2} \right). \quad (12)$$

Hence, we have

$$\frac{u_a}{U} = \frac{2}{\left(1 - \frac{a}{R}\right) \left(\ln \frac{8R}{a} - \frac{1}{2}\right)} \approx 0.49. \quad (13)$$

Thus, the axial flow velocity is approximately half of the translation velocity of the vortex ring, not a small contribution. From figure 4(b) we identify $n = 4$ crests, so we can estimate a wavelength $\lambda = 2\pi R/n = 4\pi$ and a wavenumber $k = 2\pi/\lambda = 1/2$. From equation (2.17) of Windnall and Bliss (1971), we have instability if

$$K = (ka) \frac{u_a}{u_\theta} > 2^{1/2} - 1, \quad (14)$$

where $u_\theta = \Gamma/2\pi a$ is the swirl velocity of the vortex ring. Since $ka = 1/4$ and $u_a/u_\theta = (R/a - 1)^{-1} = 1/15$, we have $K = 1/60 \ll 1$, hence we have no instability.

Higher twist values effects have been investigated too: results for $Tw = 2$ for different initial conditions are shown in figures 5 and 6. These results are in good agreement with similar behavior observed previously: for large computational times the initially twisted ring develops perturbations of larger amplitude, that appear to be proportional to the superimposed twist values. Test cases of straight vortices with $Tw (=N) = -1$ and $Tw (=N) = -2$ (with winding number $w = 1$ and $w = 2$, respectively) and opposite vorticity directions (see

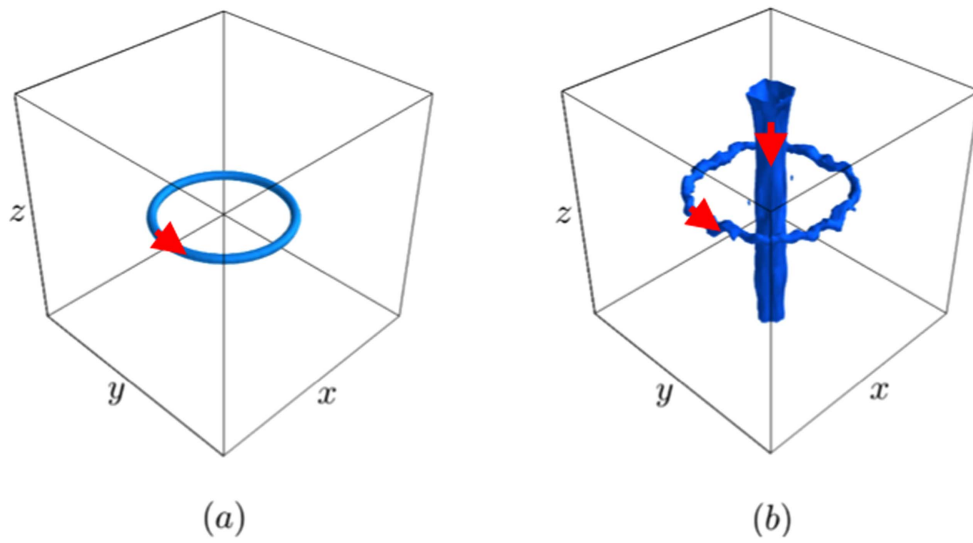


Figure 5. (a) Initial condition $t = 0$: twist $Tw = 2$ is superimposed on the vortex ring by rotating the iso-phase surface $\theta = \bar{\theta}$ by 4π around the vortex axis. (b) $t = 20$: a straight, central vortex is instantaneously generated from the very first time-step. In this case the iso-density surfaces with $\rho = 0.1$, and $a = O(\xi)$ are quite irregular.

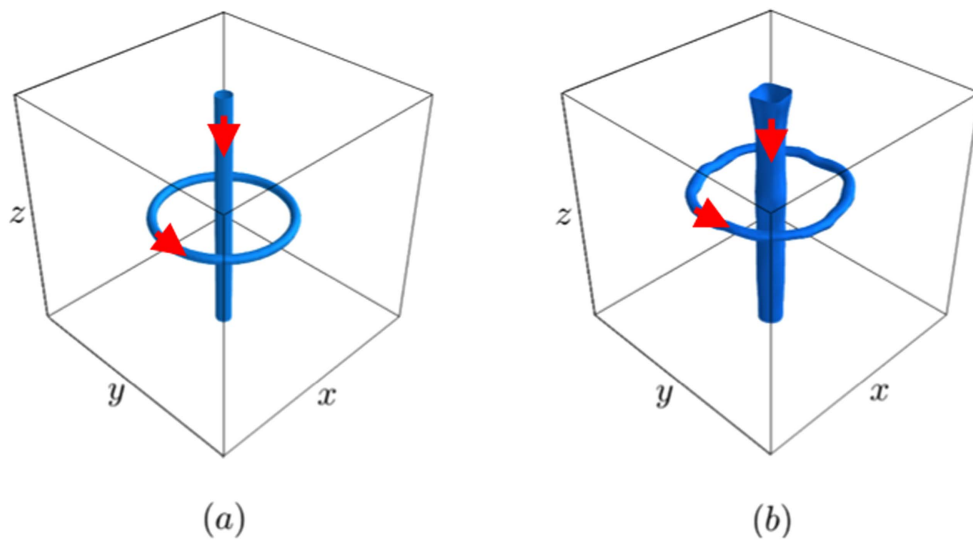


Figure 6. (a) Initial condition $t = 0$: a vortex ring and a central straight vortex are initially present; the ring has no twist, whereas the straight vortex has winding number $w = 2$. The central vortex induces a twist $Tw = 2$ on the ring (see the contour plot of figure 2(b)). (b) $t = 20$: the iso-density surfaces with $\rho = 0.1$ and $a = O(\xi)$ appear to be more regular.

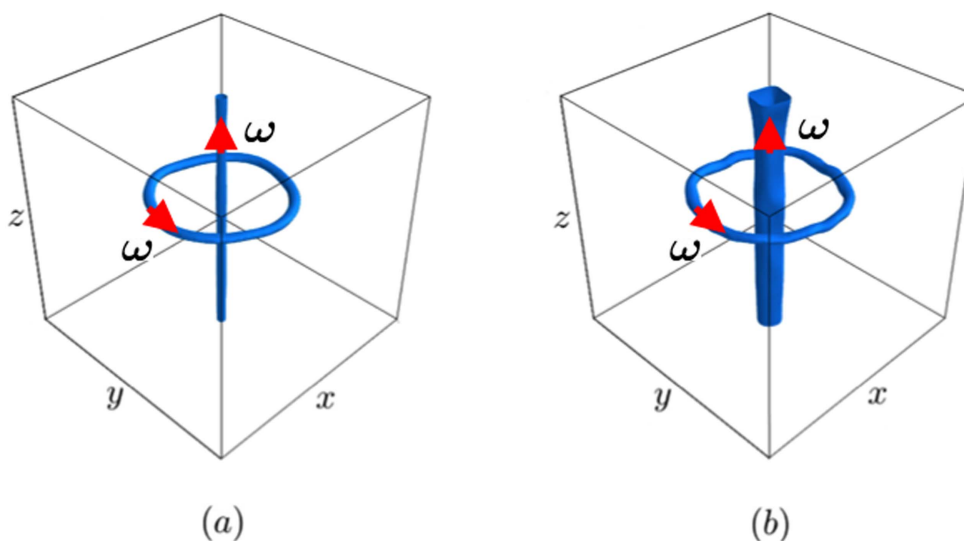


Figure 7. Evolution of a vortex ring and a central, straight vortex with $w = 1$ and $w = 2$ and vorticity upwards. Iso-density surfaces ($\rho = 0.1$) for the two cases at $t = 80$: (a) $Tw = N = -1$, $a = O(\xi/2)$; (b) $Tw = N = -2$, $a = O(\xi)$.

figure 7) have also been studied, confirming the present analysis. Note that when $w > 1$ the vortex core tends to get thicker, but it remains of the order of the healing length ξ .

5. Concluding remarks

In this paper we have shown that twist, defined purely in terms of the rotation of the iso-phase surface around the defect centerline, is a property of the system that produces physical, observable effects. These have been explored by implementing two alternative ways to generate twist. In the first case a uniform rotation of the phase has been superimposed on a planar vortex ring axis with the consequent instantaneous generation of a central straight vortex from the very first time step. The superimposed twist amounts to an axial flow acting along the ring centerline. Such an initial condition, however, seems to be quite unnatural, producing very distorted and corrugated iso-density surfaces that seem to lose coherency during time evolution. We argue that this is due to an artificial adjustment of the phase distribution, followed by a forced relaxation to a uniform background density. This state does not represent an analytical solution to the governing equation, producing irregular perturbations in the numerical solution. In the second case we consider an initially untwisted planar vortex ring with a second straight vortex placed on the central axis. The angular velocity of the straight vortex induces a uniform twist in the ring due to the natural propagation of density and phase through the ambient space. The same twist, due to the action of the vortex ring swirling flow, is also present on the straight vortex. In this case iso-density surfaces show some oscillations, but the irregularity is now typical of low amplitude and long wavelength perturbations. We show that the velocity of the induced axial flow on the vortex ring core is about half of the ring propagation velocity, with oscillations consistent with neutral stability results. This behavior has been found consistently by similar test cases analyzed for different initial conditions and twist values. Given that twist effects are evidently related to mutual

induction effects, one can argue that the direct relation that has been established between the nonlinear Schrödinger equation and the Biot-Savart operator (Bustamante and Nazarenko 2015) can be equally extended to the GPE employed here.

One other interesting aspect is the interplay of topology and physics. Since defects have no internal structure, twist cannot be associated with any internal winding of material lines. However it can be related to the uniform rotation of the iso-phase surface that, in agreement with a recent analysis (Salman 2017), influences the physics of the system. Computational evidence (Zuccher and Ricca 2015, 2017) and theoretical work (Sumners 1987, Ruzmaikin and Akhmetiev 1994, Sumners and Ricca 2017) demonstrate that defects fibered by iso-phase surfaces (Seifert surfaces) have total linking number (i.e. helicity) $Lk_{\text{tot}} = 0$. With reference to the case of figure 3 we see that the initial twist condition $T_w = 1$ artificially superimposed on the planar vortex ring (with $W_r = 0$) leads to an inconsistency given by $Lk_{\text{tot}} = 0 \neq W_r + T_w = 1$. In this case the emergence of the second straight vortex (of $W_{r_2} = 0$ and $T_{w_2} = 1$) is therefore a necessary condition: the infinitely long straight vortex being effectively linked with the vortex ring (of $W_{r_1} = 0$ and $T_{w_1} = 1$) contributes to total linking with $Lk_{12} = Lk_{21} = -1$ (according to relative orientation), so that by making use of a result demonstrated in Laing *et al* (2015), we have then

$$Lk_{\text{tot}} = 0 = W_{r_{\text{tot}}} + T_{w_{\text{tot}}} = W_{r_1} + W_{r_2} + 2Lk_{12} + T_{w_{\text{tot}}} = -2 + 2. \quad (15)$$

We should point out that induced twist does not necessarily imply generation of additional phase singularities, as is evident when we consider the folding process of a single quantum vortex loop, where the generation of new twist is naturally compensated by the spontaneous production of writhe (see for instance Zuccher and Ricca 2017). In summary, we provide evidence that not only twist is a physically relevant quantity associated with a velocity field in the system, but since twist provides an imprint of linking, the topological condition of zero helicity for the Seifert framing of phase defects implies the presence of an additional kinetic potential, in analogy with the Aharonov–Bohm effect of quantum mechanics, where the complex phase of a charged particle’s wave function is invariably associated with the physical effects of an electromagnetic potential.

ORCID iDs

Simone Zuccher  <https://orcid.org/0000-0002-9057-6892>

Renzo L Ricca  <https://orcid.org/0000-0002-7304-4042>

References

- Allen A J, Zuccher S, Caliari M, Proukakis N P, Parker N G and Barenghi C F 2014 Vortex reconnections in atomic condensates at finite temperature *Phys. Rev. A* **90** 013601
- Bustamante M D and Nazarenko S 2015 Derivation of the Biot-Savart equation from the nonlinear Schrödinger equation *Phys. Rev. E* **92** 053019
- Caliari M and Zuccher S 2016 Reliability of the time splitting Fourier method for singular solutions in quantum fluids (arXiv:1603.05022)
- Caliari M and Zuccher S 2017 INFFTM: fast evaluation of 3d Fourier series in MATLAB with an application to quantum vortex reconnections *Comput. Phys. Commun.* **213** 197–207
- Clark di Leoni P, Mininni P D and Brachet M E 2016 Helicity, topology, and Kelvin waves in reconnecting quantum knots *Phys. Rev. A* **94** 043605
- Sumners De W L 1987 Knots, macromolecules and chemical dynamics *Graph Theory and Topology in Chemistry* ed R B King and D Rouvray (Amsterdam: Elsevier) pp 3–22

- Summers De W L and Ricca R L 2017 Zero-linking, helicity, integrability and isophase surfaces in fluid systems in preparation
- Fukumoto Y and Miyazaki T 1991 Three-dimensional distortions of a vortex filament with axial velocity *J. Fluid Mech.* **222** 369–416
- Gross E P 1963 Hydrodynamics of a superfluid condensate *J. Math. Phys.* **4** 195–207
- Koplik J and Levine H 1993 Vortex reconnection in superfluid helium *Phys. Fluids* **9** 1375–8
- Laing C E, Ricca R L and Summers De W L 2015 Conservation of writhe helicity under anti-parallel reconnection *Sci. Rep.* **5** 9224
- Moffatt H K 1969 The degree of knottedness of tangled vortex lines *J. Fluid Mech.* **35** 117–29
- Moffatt H K 2014 Helicity and singular structures in fluid dynamics *PNAS USA* **111** 3663–70
- Moffatt H K and Ricca R L 1992 Helicity and the Călugăreanu invariant *Proc. R. Soc. A* **439** 411–29
- Moore D W and Saffman P G 1972 The motion of a vortex filament with axial flow *Phil. Trans. R. Soc. A* **272** 403–29
- Moreau J J 1961 Constantes d'un tourbillon en fluide parfait barotrope *Acad. Sci. Paris* **252** 2810–2
- Nelson N R 2002 *Defects and Geometry in Condensed Matter Physics* (Cambridge: Cambridge University Press)
- Pitaevskii L P 1961 Vortex lines in an imperfect Bose gas *Sov. Phys. JETP* **13** 451–4
- Ricca R L and Berger M A 1996 Topological ideas and fluid mechanics *Phys. Today* **49** 24–30
- Ricca R L and Moffatt H K 1992 The helicity of a knotted vortex filament *Topological Aspects of the Dynamics of Fluids and Plasmas* ed H K Moffatt *et al* (Dordrecht: Kluwer) pp 225–36
- Ruzmaikin A and Akhmetiev P 1994 Topological invariants of magnetic fields, and the effect of reconnections *Phys. Plasmas* **1** 331–6
- Salman H 2017 Helicity conservation and twisted Seifert surfaces for superfluid vortices *Proc. R. Soc. A* **473** 20160853
- Sullivan I S, Niemela J J, Herschberger R E and Bolster D 2008 Dynamics of thin vortex rings *J. Fluid Mech.* **609** 319–47
- Widnall S E and Bliss D B 1971 Slender-body analysis of the motion and stability of a vortex filament containing an axial flow *J. Fluid Mech.* **50** 335–53
- Zuccher S, Caliori M, Baggaley A W and Barenghi C F 2012 Quantum vortex reconnections *Phys. Fluids* **24** 125108
- Zuccher S and Ricca R L 2015 Helicity conservation under quantum reconnection of vortex rings *Phys. Rev. E* **92** 061001
- Zuccher S and Ricca R L 2017 Relaxation of twist helicity in the cascade process of linked quantum vortices *Phys. Rev. E* **95** 053109